

Maintenance decision-making model for gas turbine engine components

Hongseok Kim¹, and Do-Nyun Kim²

¹*Department of Mechanical Engineering, Seoul National University, Seoul 08826, Republic of Korea
saint4561@snu.ac.kr*

²*Department of Mechanical Engineering, Institute of Advanced Machines and Design, and Institute of Engineering Research, Seoul National University, Seoul 08826, Republic of Korea
dnkim@snu.ac.kr*

ABSTRACT

When designing gas turbine engine components, the inspection and maintenance (I&M) plan is prepared using the safe life. However, the I&M plan determined using safe life may be costly since all components are replaced at designated life. Therefore, it is important to make maintenance decisions considering the time-dependent deterioration process of gas turbine engine components for a cost-saving I&M plan. In this study, we proposed a maintenance decision-making model for gas turbine engine components based on a partially observed Markov decision process (POMDP). Using dynamic Bayesian networks, a decision-making model integrating a reliability analysis model, and a decision model for I&M planning was constructed. The signal amplitude data resulting from non-destructive inspection according to operation hour was used as partially observed data. The total cost obtained from the proposed model were compared with the results using a fixed I&M plan. The proposed model resulted in more cost-effectiveness I&M planning within affordable risk levels by considering the interaction between risk cost and I&M cost.

1. INTRODUCTION

Ensuring the safety of the gas turbine engine is very important in aircraft operation. There are two traditional inspection & maintenance (I&M) strategies to operate aircraft safely; safe life and damage tolerance design. The safe life method (C. H. Cook et al., 1982) replaces all components after the design allowable life, and time-based maintenance (TBM) (Bousdekis et al., 2015) inspects and repairs all parts at predetermined intervals. However, traditional I&M methods require high costs since I&M

actions are planned without the consideration of the components' condition. For this reason, a condition-based maintenance method that emphasizes combining data-driven reliability models with condition-monitored data was developed (Alaswad & Xiang, 2017).

Markov decision process (MDP) is one of the widely used methodologies for decision-making models with the condition-based maintenance (CBM) method. MDP takes actions at each stage to maximize the reward under perfect observation of components state. However, there are limitations for MDP that perfect observation of the components state is unrealistic (Papakonstantinou & Shinozuka, 2014b). Partially observable MDP (POMDP) quantified the uncertainty of imperfect observation by estimating the belief of state from the information obtained with the probability of observation. (Papakonstantinou & Shinozuka, 2014b, 2014a) determined the optimal life-cycle policy of concrete structures by implementing the POMDP. (Memarzadeh et al., 2014) proposed the algorithm for approximate learning and planning the Bayes-adaptive POMDP (BA-POMDP) framework to find the optimal maintenance plan of wind farms.

Morato et al. (Morato et al., 2020) incorporated the dynamic Bayesian networks (DBNs) and POMDP to obtain optimal I&M strategy for deteriorating structure. They modeled the deterioration model based on time-invariant parametric DBNs, and an optimal I&M plan was generated by minimizing the total cost of inspection, maintenance, and reliability. Hlaing et al. (Hlaing et al., 2022) presented the non-stationary policy for offshore wind tubular joints by integrating the Bayesian networks and POMDP. They estimated the probability of failure (POF) using the DBNs and obtained optimal I&M policy via POMDP.

In this work, we proposed the maintenance decision-making model for gas turbine engine components. DBNs and POMDP were integrated to get optimal I&M policy. The fatigue crack growth model was implemented for the

Hongseok Kim et al. This is an open-access article distributed under the terms of the Creative Commons Attribution 3.0 United States License, which permits unrestricted use, distribution, and reproduction in any medium, provided the original author and source are credited.

deterioration of gas turbine engine components, probability of detection (POD) curve which is a function of the crack size was used for the inspection model. The remainder of this paper is organized as follows. The decision-making model for gas turbine engine components is described in “Methodology” section. In “Numerical results”, the optimal I&M policy obtained using the proposed POMDP model is presented. In the final section, the conclusions of this study are summarized.

2. METHODOLOGY

2.1. PARTIALLY OBSERVABLE MARKOV DECISION PROCESS

MDP provides the framework that finds the optimal policy for sequential decision-making problems, as represented in Fig. 1. In Fig. 1, the circles are random state nodes, the rectangular are decision nodes, and the polygons are reward nodes. MDP determines the optimal policy that maximizes the expected reward value by using the Bellman equation as follows:

$$V^*(s) = \max_{a \in A} [R(s, a) + \gamma \sum_{s' \in S} T(s, a, s') V^*(s')] \quad (1)$$

where s is states of the system, a is the set of possible actions, and $T(s, a, s')$ is transition matrix which is the probability of transit from current state s_t to next state s_{t+1} , $R(s, a)$ is the reward when doing action a with current state s_t , and γ is discount factor employed when the problem is infinite horizon planning case (Morato et al., 2019). However, since MDP has the limitation of perfect observation, POMDP determines the optimal policy according to the belief state estimated from imperfect observation. In Fig. 2, the belief state s_t is updated from the information of component state obtained at the inspection node z_t . The optimal policy is determined at POMDP as:

$$V^*(s) = \max_{a \in A} \left[b(s)R(s, a) + \gamma \sum_{z \in Z} P(z|b, a) V^*(b') \right] \quad (2)$$

where z is observation, and b is belief state of the component. The belief state b with action m at stage n is ${}^m b^n = b^n \times A_m$, the belief state b^{n+1} at the stage $n+1$ is updated with degradation model D ; $b^{n+1} = {}^m b^n \times D$ (Faddoul et al., 2013).

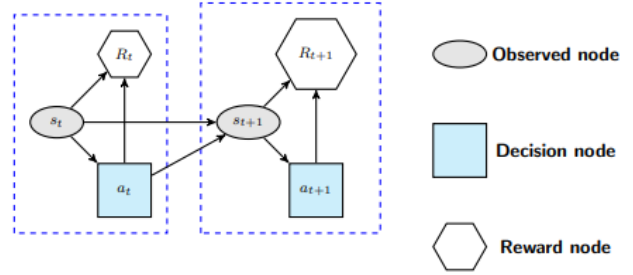


Figure 1. Graphical model for Markov decision process

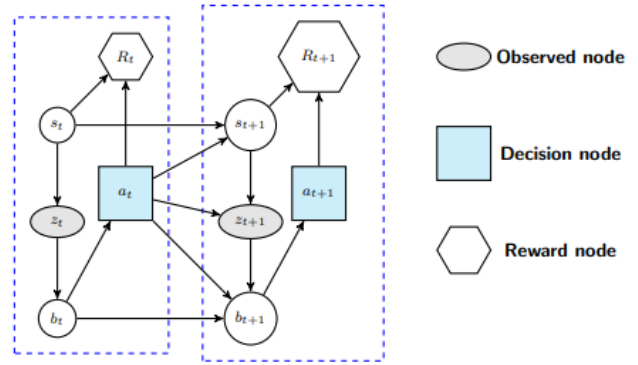


Figure 2. Graphical model for Partially observable MDP

2.2. DETERIORATION AND INSPECTION MODEL

Paris' law was used for fatigue crack deterioration model of gas turbine engine component as:

$$\frac{da}{dN} = C(\Delta K)^m \quad (3)$$

where a is the size of crack, N is the cycles of loads, ΔK is the stress intensity factor range which is function of crack size, shape, and stress range $\Delta\sigma$, and C and m are the constants related to material property.

Eddy current inspection (ECI), one of the non-destructive inspection (NDI) methods, was used as partial observation model to update the belief state of the gas turbine engine component. The POD of ECI depends on the crack size and the detection threshold (Hlaing et al., 2022). The size of the crack is estimated from the ECI signal amplitude in Eq. (4), and the POD is calculated from Eq. (5). Figure 3 presents the relation curve between the signal amplitude and the crack length, and Fig. 4 is the probability of detection (POD) estimated from the detection result data of NDI personnel (D. Lee & Kwon, 2023). The $a_{50/95} = 1.123$ in Fig. 4 means that the detectable crack size at a 50% probability with 95% confidence is 1.123mm. The size of the crack is estimated

from the ECI signal amplitude in Eq. (4), and the POD is calculated from Eq. (5).

$$\hat{a} = \beta_0 + \beta_1 a + \varepsilon \tag{4}$$

$$POD(a) = \frac{aa^\gamma}{1 + aa^\gamma} \tag{5}$$

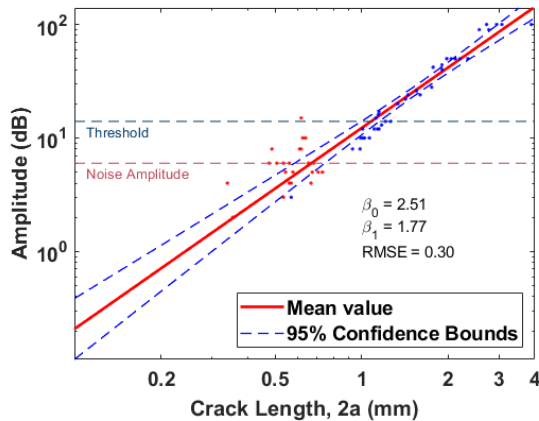


Figure 3. Relation between ECI signal and crack size

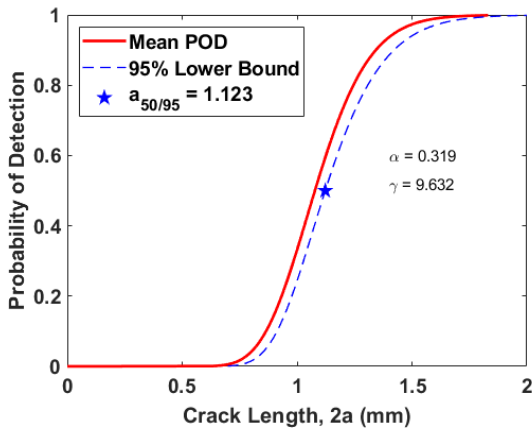


Figure 4. Probability of detection curve

2.3. DECISION-MAKING MODEL BASED ON DYNAMIC BAYESIAN NETWORKS

The maintenance decision-making model based on Dynamic Bayesian Networks (DBNs), depicted in Fig. 5 was developed by incorporating the deterioration, inspection model, and POMDP described above. In Fig. 5, the initial nodes have no parent nodes, the static nodes are time-independently invariant nodes, the observed node obtains evidence, the functional nodes formulate the crack length distribution and reliability, the decision nodes decide for actions, and the cost of the decision incurred in the utility nodes. The continuous operation time is discretized into time slices with uniform intervals.

Table 1. Prior probability distributions of initial nodes

Var	Distribution	Mean	SD	Corr.
$m, \ln(C)$	Binormal	$(2.5, \log(5.2 \times 10^{-12}))$	$(0.3, 0.47)$	-0.9
$\Delta\sigma$ (MPa)	Normal	40	5	-
a_0 (mm)	Lognormal	-1.0	0.001	-
a_r (mm)	Lognormal	-1.0	0.001	-
Y_n (%)	Normal	3.29	2.86	-

First, the crack length distribution at time slice $t-1$ (a_{t-1}) is estimated in the deterioration model using $\Delta\sigma, m$, initial crack length at time slice $t-1$ (a_{t-1}^0). Next, a_{t-1} is updated to a_{t-1}^* based on the actions determined by the signal amplitude node Y_{t-1} , noise amplitude Y_n , decision nodes for inspection DZ , the threshold of inspection D_{th} , and maintenance DM . The updated crack length distribution at time slice $t-1$ a_{t-1}^* is used as initial crack length distribution a_t^0 at time slice t . The prior distributions of initial nodes are presented in Table 1.

The actions determined in each decision node are as follows: The inspection decision determines whether to perform an inspection or not. The cost of the inspection is obtained in inspection utility node UZ depending on the result of the inspection decision.

- No-inspection: the crack length states transit according to the deterioration model.

- Inspection: binary inspection result is obtained at node Z as ‘detected’ or ‘not detected’. When the inspection result is ‘detected’, the probability of failure increases as the belief state of crack length larger than the inspection threshold increase. On the other hand, the probability of failure decreases since the crack length distribution smaller than the inspection threshold rise in the case of ‘not detected’.

The quality of NDI is determined in the threshold decision node. The inspection quality is high as the threshold is lower. If the signal amplitude obtained at the cracks is larger than the inspection threshold, those cracks are detected at inspection result node Z . There is no cost for threshold decision.

There are binary options in the maintenance decision node; repair or do-nothing. The maintenance utility node UM calculates the cost of maintenance.

- Do-nothing: there is no maintenance action planned in this case, the crack length state evolves according to the stochastic deterioration process.

- Repair: perfect maintenance action is performed. The crack length distribution a_{t-1}^* is replaced by the belief state of repair crack a_r .

The total cost at time t is calculated by summing the cost of the failure, inspection, and maintenance determined according to the results of each decision node as follows:

$$C_T(h) = \sum_{t=t_0}^{t_n} [C_I(t)\gamma + C_M(t)\gamma + P_f(t)C_f(t)\gamma] \quad (6)$$

where C_T is total cost, h is pre-defined heuristic schedule, t_n is total time horizon, C_I is inspection cost, C_M is maintenance cost, P_f is probability of failure estimated at node R , and C_f is failure cost determined in utility node UR . The C_I and C_M is not incurred in the case of no-inspection and do-nothing, respectively. The optimal actions were determined by minimizing the total cost.

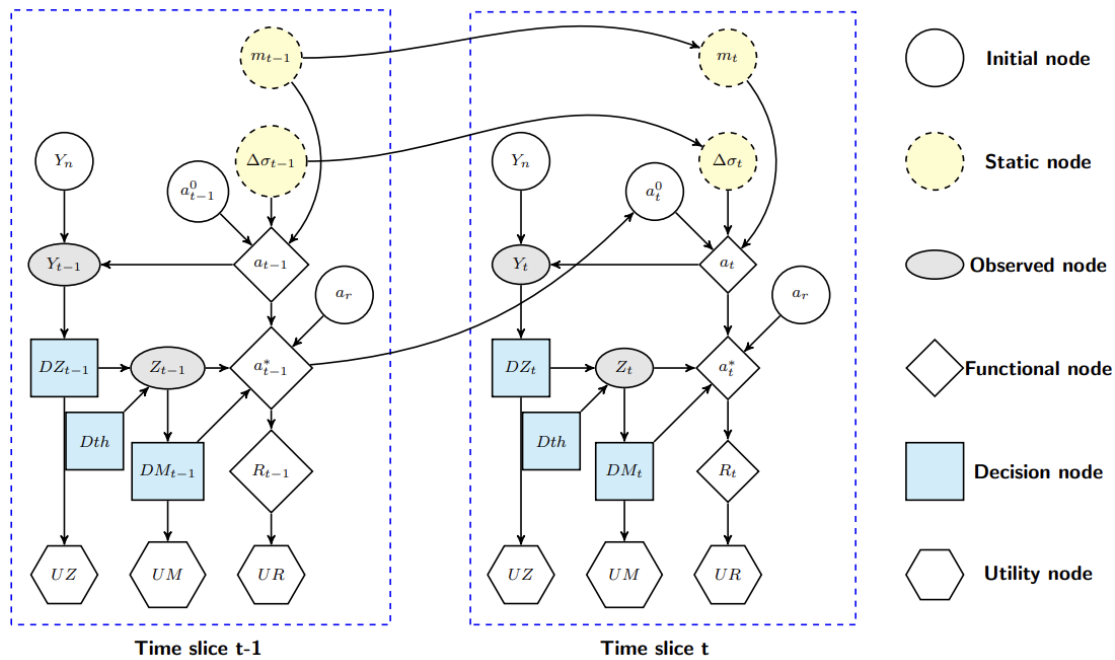


Figure 5. Maintenance decision-making model for gas turbine components

3. NUMERICAL RESULT

A maintenance decision-making model based on POMDP was constructed for the J85 gas turbine engine compressor first-stage rotor blade for the F-5 aircraft. The J85 gas turbine engine compressor first-stage rotor blade is mounted with a disc using tangs. The stress concentration at the center tang occurred due to contact force between the retainer pin and an inner surface of the tang (B. W. Lee et al., 2011). Since the fracture at the center tang may occur due to the fatigue crack initiated from fretting damages by contact stress, it is important to optimize the I&M planning of the blade center tang.

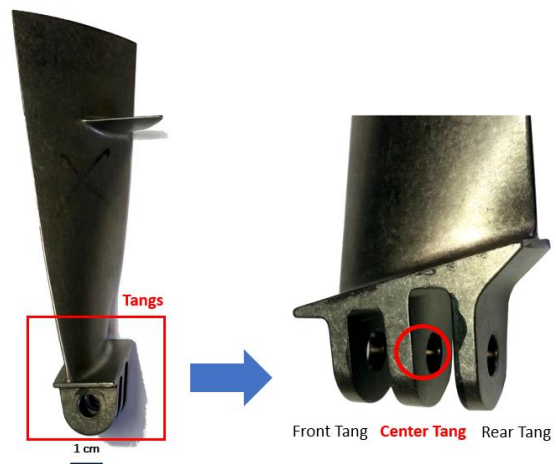


Figure 6. J85 engine compressor first-stage blade

3.1. DISCRETIZATION SCHEMES FOR MODEL PARAMETERS

Discretization of each random variable is necessary in POMDP since the probability of partial observation is discretized (Morato et al., 2020). The accuracy of POF and computational efficiency are affected by the discretization scheme. The discretization schemes for each variable in Fig. 5 are presented in Table 2. The random variables were discretized with a small number of discretization states for computational costs.

Table 2. Discretization schemes

Var	Interval Boundaries
a, a_r	$0, \exp(\log(0.01):(\log(3)-\log(0.01))/4:\log(3)), \inf$
m	$0, \log(\exp(1):(\exp(3.9)-\exp(1))/4:\exp(3.9)), \inf$
$\Delta\sigma$	$1:60/4:60, \inf$
Y_n, Y	$0:6:100$

3.2. OPTIMAL POLICY BASED ON DECISION-MAKING MODEL

The overall cost of utilizing the proposed decision-making model was compared with that of time-based maintenance (TBM), a traditional I&M strategy. In TBM, NDI is conducted for every time slice, and when a crack is detected, a perfect repair action is performed. On the other hand, the decision to execute NDI and repair is made for each time slice in the most cost-effective way in the decision-making model. The parametric study for the costs of inspection, maintenance, and failure was conducted to specify the effects of actions. The state of the measured signal amplitude Y was imported from the actual measured data at each time slice (D. Lee & Achenbach, 2016). If the inspection threshold is smaller than the measured signal amplitude, it is observed that a crack is detected, and a perfect repair action is performed in the TBM strategy. Otherwise, in the POMDP strategy, it is determined whether to perform inspection and maintenance actions for each time slice depending on the total cost.

The ratio of total cost between TBM and POMDP depending on the NDI threshold over 5 time slices is shown in Fig. 7. The evidence indicated the crack state progressed from state 2 to state 5 in each time slice, with failure occurring at state 6. After repair action, the crack state returned to state 2. R_{MI} is the ratio of cost between inspection and maintenance, R_{FM} is the ratio of cost between failure and maintenance, and R_C is the total cost ratio between TBM and POMD as:

$$R_{MI} = \frac{C_M}{C_I}, R_{FM} = \frac{C_F}{C_M} \quad (7)$$

$$R_C = 100 \frac{C_{POMDP} - C_{TBM}}{C_{TBM}} (\%) \quad (8)$$

Where C_M is the cost of maintenance, C_I is the cost of inspection, C_F is the cost of failure, C_{POMDP} is total cost for POMDP, and C_{TBM} is that of TBM. The $R_{MI} = [10, 20, 30, 40, 50]$, and $R_{FM} = [100, 50, 25, 20]$ were used to estimate the total cost. The C_{POMDP} is more cost-effective than C_{TBM} when the total cost ratio is a negative value; conversely, if this ratio is a positive value, the C_{TBM} is less expensive than C_{POMDP} .

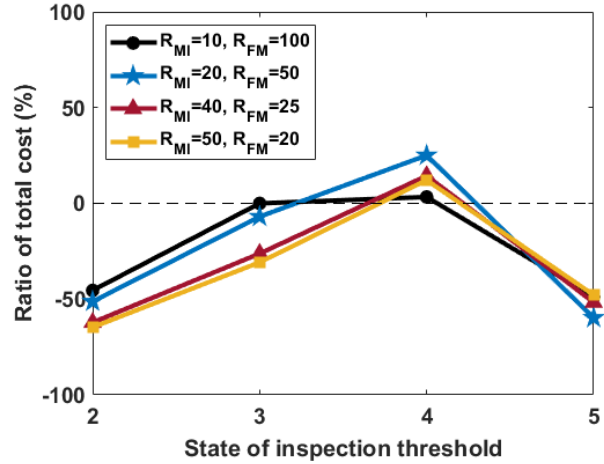


Figure 7. Ratio of total cost between TBM and POMDP

The cost of the POMDP strategy is cheaper than TBM in all R_{MI} and R_{FM} when the threshold of inspection is lower than 4. This implies that a high-quality inspection is crucial for an I&M strategy based on POMDP. When the inspection quality is high ($D_{th} = 2, 3$), the crack state is identified early. This enables decisions on whether to perform inspections and repairs based on the state of crack growth. Consequently, the POMDP strategy conducts fewer inspections and repairs compared to the TBM strategy, and no preventative repairs, resulting in lower total costs as illustrated in Fig. 8.

When $D_{th} = 4$, the crack state is detected before it grows near the limit state. In the TBM strategy, after detecting the crack, repairs are performed to maintain a low probability of failure. The inspections following repair prevent the crack from propagating toward the limit state, resulting in a low cost of failure. On the other hand, in the POMDP strategy, when the R_{MI} is low, more repairs are carried out than TBM due to lower inspection quality. When R_{MI} is high, the probability of failure increases because inspections are not performed after repairs, leading to a higher total cost.

Also, the ratio of total cost R_C increases as the inspection threshold decreases. Exceptionally, when using the TBM strategy with $D_{th}=5$, R_C increases. This occurs as the crack is detected in state 5, which is proximate to the failure state, as depicted in Figure 8(a). Consequently, the estimated probability of failure is relatively high, leading to an increased total cost. On the other hand, when using the POMDP strategy, repairs were carried out preventatively

even if the inspection result indicated ‘No-detected’ as shown in Fig. 8(b), owing to the limited inspection quality. Therefore, when the inspection threshold is 5, the total cost of the POMDP strategy was relatively lower than that of TBM since the failure cost of the POMDP strategy was low through preventive repairs.

Fig. 8 presents the optimal actions determined by using TBM and POMDP strategy depending on each R_{MI} and R_{FM} during 5 time slices. There are two color blocks to describe the results of the decision at each time slice; the left is inspection, and the right is maintenance. The action types of inspection are ‘No-inspection’ (gray colors), ‘No-detected’ (sky colors), and ‘Detected’ (blue colors). The red colors mean the case of a ‘Repair’ action, and the orange colors indicate a ‘Do-nothing’ action.

In the context of inspection and maintenance, Fig. 8 illustrates how the cost ratio impact the frequency of inspection and maintenance. Specifically, when the cost ratio of inspection and maintenance R_{MI} is relatively small compared to the cost of failure and maintenance R_{FM} (Fig. 8(b), (c)), more frequent inspection were performed. Since the cost of the failure is expensive compare to inspection and maintenance, it is more cost-effective to identify the state of the crack length early by inspecting frequently. For example, the optimal decision for inspection of $R_{MI}=10$, and $R_F=100$ was to inspect every time slice, similar to the TBM strategy.

In the case of high R_{FM} , and high D_{th} , repair action was performed even in the case of ‘No-detected’. Since the cost of maintenance is cheaper than that of failure, and the result of inspection is uncertain, this policy is optimal to reduce the POF. On the other hand, when the information quality of inspection was high ($D_{th} \leq 3$), repair action was not performed immediately, even though the result of the inspection was ‘Detected’. In this case, the decision to repair or not can be determined by the condition of the crack, not preventatively. When R_{MI} is larger than R_{FM} (Fig. 8(d), (e)), the cost of maintenance becomes expensive. The preventive inspections and maintenance were reduced due to high-cost maintenance. Therefore, the inspection was not performed at the first time slice for all inspection thresholds. The total cost ratio R_c was highest when $R_{MI}=50$, $R_{FM}=20$, and $D_{th} = 2$, as presented in Fig. 7. The findings from Figures 7 and 8 indicate that an increase in inspection quality and a decrease in the cost ratio between maintenance and repair enhance the effectiveness of the maintenance decision-making model based on POMDP.

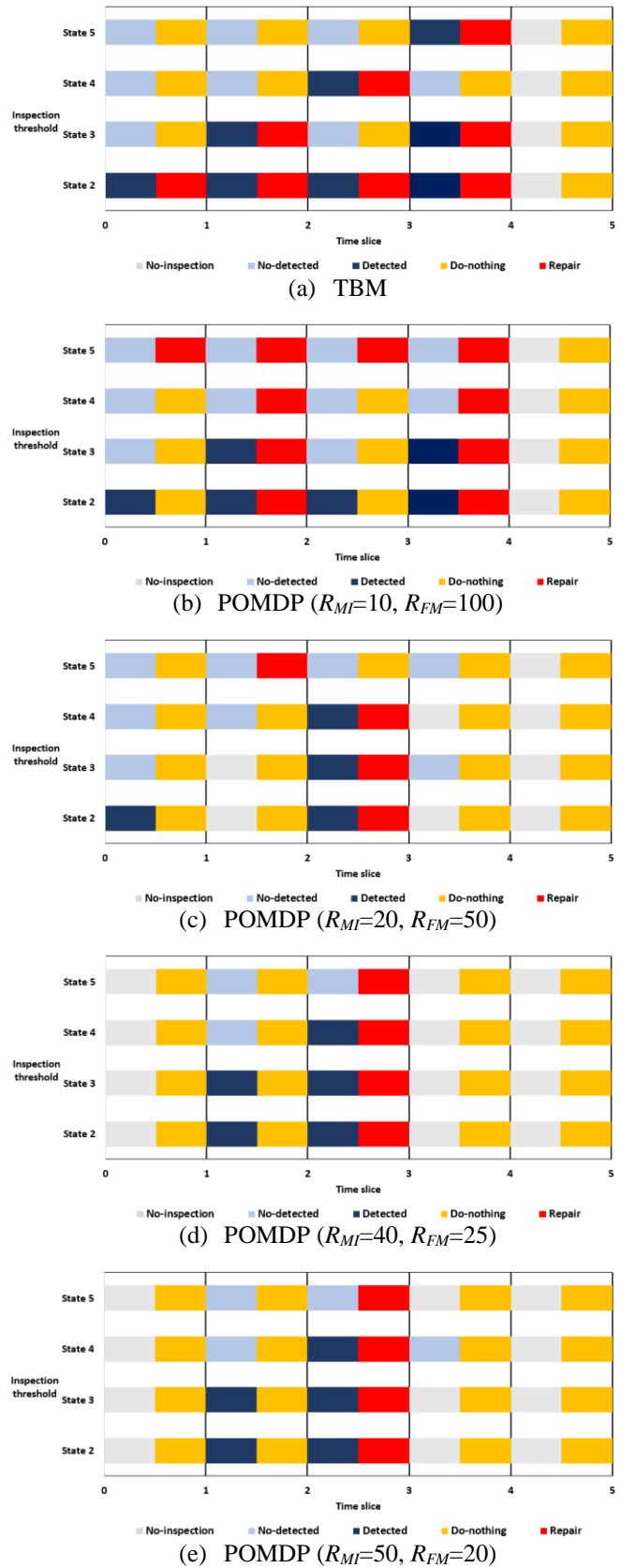


Figure 8. Optimal actions of TBM and POMDP

4. CONCLUSION

In this work, we proposed a maintenance decision-making model for gas turbine components based on POMDP. DBNs and POMDP were integrated to construct the maintenance decision-making model. The fatigue crack growth model was implemented for deterioration of gas turbine engine components, POD curve was used for the inspection model. The total cost of POMDP was lower than that of TBM when inspection quality was high. Also, it was proven that the maintenance decision-making model is more effective than TBM as the cost ratio between maintenance and repair is smaller by parametric study of cost ratio.

Our future work will focus on complicate inspection and maintenance actions. The various options for inspection and maintenance actions will improve the decision-making model more elaborately.

ACKNOWLEDGEMENT

This work was supported by Korea Research Institute for Defense Technology Planning and Advancement (KRIT) Grant funded by Defense Acquisition Program Administration (DAPA) (No. 21-107-E00-012-02).

REFERENCES

Alaswad, S., & Xiang, Y. (2017). A review on condition-based maintenance optimization models for stochastically deteriorating system. *Reliability Engineering and System Safety*, 157, 54–63. <https://doi.org/10.1016/j.res.2016.08.009>

Bousdekis, A., Magoutas, B., Apostolou, D., & Mentzas, G. (2015). A proactive decision making framework for condition-based maintenance. *Industrial Management and Data Systems*, 115(7), 1225–1250. <https://doi.org/10.1108/IMDS-03-2015-0071>

C. H. Cook, C. E. Spaeth, D. T. Hunter, & R. J. Hill. (1982, April). Damage Tolerant Design of Turbine Engine Disks. *Turbo Expo: Power for Land, Sea, and Air*. <https://doi.org/https://doi.org/10.1115/82-GT-311>

Faddoul, R., Raphael, W., Soubra, A.-H., & Chateaneuf, A. (2013). Incorporating Bayesian Networks in Markov Decision Processes. *Journal of Infrastructure Systems*, 19(4), 415–424. [https://doi.org/10.1061/\(asce\)is.1943-555x.0000134](https://doi.org/10.1061/(asce)is.1943-555x.0000134)

Hlaing, N., Morato, P. G., Nielsen, J. S., Amirafshari, P., Kolios, A., & Rigo, P. (2022). Inspection and maintenance planning for offshore wind structural components: integrating fatigue failure criteria with Bayesian networks and Markov decision processes. *Structure and Infrastructure Engineering*, 18(7), 983–1001. <https://doi.org/10.1080/15732479.2022.2037667>

Lee, B. W., Suh, J., Lee, H., & Kim, T. gu. (2011). Investigations on fretting fatigue in aircraft engine compressor blade. *Engineering Failure Analysis*, 18(7), 1900–1908. <https://doi.org/10.1016/j.engfailanal.2011.07.021>

Lee, D., & Achenbach, J. D. (2016). Analysis of the Reliability of a Jet Engine Compressor Rotor Blade Containing a Fatigue Crack. *Journal of Applied Mechanics, Transactions ASME*, 83(4). <https://doi.org/10.1115/1.4032376>

Lee, D., & Kwon, K. (2023). Dynamic Bayesian network model for comprehensive risk analysis of fatigue-critical structural details. *Reliability Engineering and System Safety*, 229. <https://doi.org/10.1016/j.res.2022.108834>

Memarzadeh, M., Asce, A. M., Pozzi, M., & Kolter, J. Z. (2014). *Optimal Planning and Learning in Uncertain Environments for the Management of Wind Farms*. [https://doi.org/10.1061/\(ASCE\)CP](https://doi.org/10.1061/(ASCE)CP)

Morato, P. G., Nielsen, J. S., Mai, A. Q., & Rigo, P. (2019, May). POMDP based Maintenance Optimization of Offshore Wind Substructures including Monitoring. *ICASP13*. <https://doi.org/https://doi.org/10.22725/ICASP13.067>

Morato, P. G., Papakonstantinou, K. G., Andriotis, C. P., Nielsen, J. S., & Rigo, P. (2020). *Optimal Inspection and Maintenance Planning for Deteriorating Structural Components through Dynamic Bayesian Networks and Markov Decision Processes*. <https://doi.org/10.1016/j.strusafe.2021.102140>

Papakonstantinou, K. G., & Shinozuka, M. (2014a). Planning structural inspection and maintenance policies via dynamic programming and Markov processes. Part II: POMDP implementation. *Reliability Engineering and System Safety*, 130, 214–224. <https://doi.org/10.1016/j.res.2014.04.006>

Papakonstantinou, K. G., & Shinozuka, M. (2014b). Planning structural inspection and maintenance policies via dynamic programming and Markov processes. Part I: Theory. *Reliability Engineering and System Safety*, 130, 202–213. <https://doi.org/10.1016/j.res.2014.04.005>